

PVP2013-97455

**MEASUREMENT OF FATIGUE CRACK GROWTH RATES FOR SA-372 GR. J STEEL
IN 100 MPA HYDROGEN GAS FOLLOWING ARTICLE KD-10**

Brian Somerday
Sandia National Laboratories
Livermore, CA, USA

Chris San Marchi
Sandia National Laboratories
Livermore, CA, USA

Kevin Nibur
Hy-Performance Materials
Testing, LLC
Bend, OR, USA

ABSTRACT

The objective of this work is to enable the safe design of hydrogen pressure vessels by measuring the fatigue crack growth rates of ASME code-qualified steels in high-pressure hydrogen gas. While a design-life calculation framework has recently been established for high-pressure hydrogen vessels, a material property database does not exist to support the analysis. This study addresses such voids in the database by measuring the fatigue crack growth rates for three heats of ASME SA-372 Grade J steel in 100 MPa hydrogen gas at two different load ratios (R). Results show that fatigue crack growth rates are similar for all three steel heats and are only a mild function of R . Hydrogen accelerates the fatigue crack growth rates of the steels by at least an order of magnitude relative to crack growth rates in inert environments. Despite such dramatic effects of hydrogen on the fatigue crack growth rates, measurement of these properties enables reliable definition of the design life of steel hydrogen containment vessels.

INTRODUCTION

One of the safety issues related to containment of high-pressure hydrogen gas is the phenomenon of hydrogen embrittlement of structural materials. Hydrogen embrittlement is manifested in materials by reduced resistance to crack propagation, e.g., subcritical cracking thresholds less than the fracture toughness and accelerated rates of fatigue crack growth. As a result, the structural integrity of hydrogen containment components can be compromised. Although materials such as structural steels can exhibit quite pronounced

effects of hydrogen embrittlement, such susceptibility to hydrogen embrittlement does not preclude the materials from consideration in hydrogen containment components. Rather, design-life calculations that accommodate hydrogen embrittlement can be applied to hydrogen containment components.

A design-life calculation that accommodates hydrogen embrittlement was recently established for high-pressure hydrogen vessels. This method was published as Article KD-10 ("Special Requirements for Vessels in High Pressure Gaseous Hydrogen Transport and Storage Service") in Section VIII, Division 3 of the ASME Boiler and Pressure Vessel Code [1, 2]. The design-life calculation in Article KD-10 is effective in addressing hydrogen embrittlement for the following reasons. First, the structural failure mode facilitated by hydrogen embrittlement is explicitly identified. In the case of pressure vessels subjected to pressure cycling, the governing failure mode is expected to be hydrogen-accelerated fatigue crack growth. Second, once this life-limiting failure mode is identified, the appropriate analysis and material-property inputs for quantifying the design life can be applied. In this case, the design-life analysis requires the fatigue crack growth rate (da/dN) vs. stress-intensity factor range (ΔK) relationship for the structural steel in the service environment, i.e., high-pressure hydrogen gas.

The objective of this work is to enable the safe design of hydrogen pressure vessels by measuring the fatigue crack growth rates of ASME code-qualified steels in high-pressure hydrogen gas. One class of steels currently used for hydrogen gas vessels is the ASME SA-372 series. These steels are

candidates for higher-pressure hydrogen containment vessels with service pressures up to 100 MPa. While ASME Article KD-10 provides a design-life framework for these high-pressure vessels, a material property database does not exist to enable the analysis. This study addresses such voids in the database by measuring the da/dN vs. ΔK relationship for an ASME SA-372 steel in 100 MPa hydrogen gas.

NOMENCLATURE

a	Crack length or crack depth
a_c	Critical crack depth
a_f	Final crack length
a_o	Initial crack length or crack depth
m	Exponent in fatigue crack growth relationship
A	Parameter in algorithm for increasing load test
C	Constant in fatigue crack growth relationship
da/dN	Crack growth rate (crack extension per load cycle)
El	Elongation
HSLA	High strength low alloy
K_f	Final maximum stress-intensity factor
K_{max}	Maximum stress-intensity factor
K_o	Initial maximum stress-intensity factor
N	Number of load cycles
N_c	Number of cycles at the critical crack depth
R	Load ratio (minimum load/maximum load)
S_u	Ultimate tensile strength
S_y	Yield strength
ΔK	Stress-intensity factor range

EXPERIMENTAL PROCEDURES

Three different heats of steel were tested in this study, where the alloy composition, heat treatment, and mechanical properties of the steels conformed to the ASME SA-372 standard, "Specification for Carbon and Alloy Steel Forgings for Thin-Walled Pressure Vessels". The steels were manufactured to meet the alloy composition requirements for Grade J, which are listed in Table 1. The SA-372 steels are typically formed into seamless pipe, and qualification of the steel is performed on test rings removed from the seamless pipe. In this study, the SA-372 Grade J test rings were heat treated to qualify the steel as Class 70. The 61 cm-long test rings were heat treated using a one-sided quench followed by tempering. The tempering temperatures and mechanical properties measured for the three steels are summarized in Table 2. The mechanical property requirements for Class 70 steels are also included in Table 2, which indicates that the three steels qualified as Class 70.

Fatigue crack growth rate testing on the SA-372 Grade J steels was conducted following guidance in ASTM Standard E647-05 [3]. The test specimens were extracted from the steel test rings and designed according to the compact tension (CT) geometry. These specimens had the following dimensions: thickness = 6.3 mm; width = 26 mm; and precrack-starter notch length = 5.2 mm. The precrack-starter notch of the CT

specimens was oriented parallel to the longitudinal axis of the seamless pipe.

TABLE 1
ASME SA-372 GR. J STEEL COMPOSITION RANGE (WT%)*

Cr	Mo	Mn	Si	C	S	P
0.80-1.15	0.15-0.25	0.75-1.05	0.15-0.35	0.35-0.50	<0.025	<0.025

*Composition balance is Fe

TABLE 2
MECHANICAL PROPERTIES FOR SA-372 GR. J STEELS

Steel	Tempering Temperature (°C)	S_u (MPa)	S_y (MPa)	El (%)
Class 70*	>595	825-1000	>485	>18
Heat 1	660	839	642	22.0
Heat 2	657	871	731	19.3
Heat 3	657	908	784	24.0

*Standard specifications

The CT specimens were prepared for testing by first cleaning the as-machined specimens in either ethanol or isopropyl alcohol. Following procedures in ASTM Standard E647-05 [3], a precrack was propagated from the starter notch in each specimen by applying cyclic loading. This precracking process was conducted in air under the following mechanical conditions: load-cycle frequency = 15 Hz; ratio of minimum load to maximum load (R) = 0.1; and final maximum stress-intensity factor (K_{max}) = 12 MPa·m^{1/2}. The average precrack was propagated a distance of 2.1 mm from the notch tip to create a total precrack length-to-width ratio of 0.278.

Fatigue crack growth tests were conducted on the SA-372 Grade J compact tension specimens in hydrogen gas using a customized laboratory apparatus consisting of a pressure vessel inserted into the load train of a servo-hydraulic mechanical test frame. Each precracked CT specimen was placed in the pressure vessel and coupled to a pull rod penetrating through the bottom cover of the vessel. The pressure vessel was equipped with spring-energized, Teflon® U-cup seals to prevent gas leakage between the pull rod and bottom cover bore. After the pressure vessel was assembled with the CT specimen inside, residual gas (e.g., air) was removed from the gas distribution manifold and pressure vessel using the following procedure: three consecutive purges with high-purity helium gas (21 MPa pressure), one evacuation, then three final consecutive purges with high-purity hydrogen gas (21 MPa pressure). The pressure vessel was then filled with hydrogen gas (99.9999% purity) to the test pressure of 100 MPa. No net load was applied to the CT specimen resulting from gas pressure acting on the end of the pull rod, since a secondary pressure chamber was designed into the vessel to ensure an equal and opposing force was applied to the pull rod. All

testing was conducted at ambient temperature (approximately 295 K).

The fatigue crack growth tests in hydrogen gas were executed following two related procedures outlined in ASTM Standard E647-05 [3]. These procedures involved either cycling the CT specimens under fixed minimum and maximum loads (i.e., constant load amplitude) or increasing maximum load following the algorithm $K_f = K_o \exp[A(a_f - a_o)]$, where K_o and K_f are the initial and final maximum stress-intensity factors, respectively, and a_o and a_f are the initial and final crack lengths, respectively. In the current study, the parameter, A , was set at values between 0.18 and 0.20 mm^{-1} . For each test method, the ratio of minimum load to maximum load (or minimum K to maximum K), R , was equal to 0.2 or 0.5 and the load-cycle frequency was 0.1 Hz (see summary in Table 3). Both loading formats led to increasing values of stress-intensity factor range (ΔK) as the crack extended. The loading and unloading rates were programmed to be constant in each cycle (i.e., triangular loading wave form) using an internal load cell as the feedback transducer in the control loop. Since the Teflon® seals impose friction forces on the pull rod, the internal load cell ensured that loads applied to the specimen were measured directly. The crack-opening displacement was measured using a linear variable differential transformer (LVDT) attached to the front face of the CT specimen. Crack extension was quantified using the unloading compliance method. Load, crack-opening displacement, and crack length data were digitally recorded at crack extension intervals of 0.13 mm. A commercial fatigue crack growth software product was used to control both the programmed loading and data acquisition.

**TABLE 3
FATIGUE CRACK GROWTH TEST SUMMARY**

Steel	Specimen No.	R	Test Method	H ₂ Gas Impurities (vppm)
Heat 1	K236-1J	0.5	fixed loads	no sample
Heat 1	K236-1K	0.2	fixed loads	O ₂ < 0.5 H ₂ O < 0.5
Heat 2	Y046-7	0.5	fixed loads	no sample
Heat 2	Y046-8	0.2	fixed loads	no sample
Heat 2	Y046-9	0.5	increasing loads	O ₂ = 6.6 H ₂ O < 0.5
Heat 3	D535-5	0.5	fixed loads	O ₂ = 2.6 H ₂ O = 0.8
Heat 3	D535-6	0.2	fixed loads	no sample
Heat 3	K236-2F	0.5	increasing loads	no sample

At the completion of each fatigue crack growth test, the crack growth rate, da/dN , was calculated by applying the incremental polynomial method in ASTM E647-05 [3] to the

crack length, a , vs. load-cycle, N , data.¹ For each da/dN value, the associated ΔK was calculated from the crack length and load range at the mid-point of the evaluated crack extension interval.

One variable that received particular attention was the actual composition of the hydrogen test gas. Although the high-purity source gas was certified as 99.9999%, some oxygen and water vapor contamination of the test gas was expected since residual air cannot be completely removed from the pressure vessel. At the termination of three individual tests (see Table 3), gas samples from the pressure vessel were collected in evacuated stainless steel bottles and were sent to a commercial laboratory for analysis. These results showed that oxygen levels were variable but did not exceed 7 vppm and water vapor was consistently less than 1 vppm.

RESULTS AND DISCUSSION

Fatigue crack growth rate data are typically plotted as the crack growth increment per cycle, da/dN , vs. the stress-intensity factor range, ΔK , on logarithmic coordinate axes. Such da/dN vs. ΔK plots for the three heats of SA-372 Grade J steel tested in 100 MPa hydrogen gas are shown in Fig. 1. The plots exhibit the expected positive slope and a linear relationship between $\log(da/dN)$ and $\log(\Delta K)$ over most of the ΔK range. This relationship between da/dN and ΔK is conventionally described by the function:

$$\frac{da}{dN} = C \Delta K^m \quad (1)$$

where C and m are constants that depend on the material and test environment. The C and m values calculated from curve fits to the da/dN vs. ΔK data are provided in Table 4. At the lower end of the ΔK range in the data sets from Fig. 1, the crack growth rates deviate from the prevailing relationship, decreasing toward the rates measured in air. This transition in crack growth rates as ΔK decreases is commonly observed for steels in hydrogen gas [4]. Between these transition points, crack growth rates are also described by Eq. (1).

The fatigue crack growth rate relationships in Fig. 1 exhibit several notable trends. First, each steel data set in hydrogen gas shows fatigue crack growth rates that are at least one order of magnitude higher than crack growth rates in air. (The da/dN vs. ΔK relationship for HSLA steels in air is from ASME Article KD-4.) Such elevated fatigue crack growth rates are a manifestation of hydrogen embrittlement. Second, some variation of the fatigue crack growth rates in hydrogen gas are

¹ The crack length data furnished by the unloading compliance method were corrected based on post-test optical measurements of the precrack and final crack lengths from the fracture surfaces. The difference between the crack lengths determined from unloading compliance and optical measurements were approximately 10-20% for the precrack and < 1% for the final crack length. A routine in the analysis software linearly corrected the unloading compliance data so that the initial and final crack lengths equaled the optically measured values.

observed among the three steel heats at $R = 0.2$ but not at $R = 0.5$. At this higher R ratio, the da/dN vs. ΔK relationships for all steel heats essentially coincide. Third, the fatigue crack growth rates in hydrogen gas depend modestly on R . At a fixed value of ΔK , crack growth rates mildly increase as R increases. Finally, the da/dN vs. ΔK relationships in hydrogen gas do not depend on the test method, i.e., constant load amplitude vs. increasing maximum load.

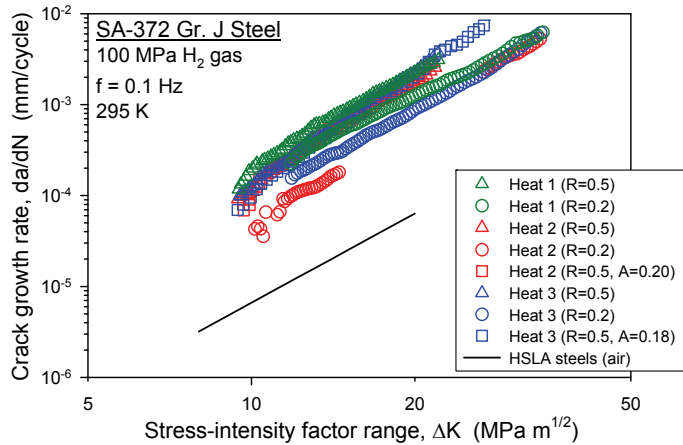


FIG. 1 FATIGUE CRACK GROWTH RATE RELATIONSHIPS FOR SA-372 GR. J STEEL IN 100 MPa HYDROGEN GAS

TABLE 4 FATIGUE CRACK GROWTH RELATIONSHIP PARAMETERS

Steel	Specimen No.	R	C (mm/cycle)· (MPa m ^{1/2}) ^{-m}	m
Heat 1	K236-1J	0.5	7.7×10^{-8}	3.4
Heat 1	K236-1K	0.2	2.2×10^{-7}	2.9
Heat 2	Y046-7	0.5	1.6×10^{-8}	3.9
Heat 2	Y046-8	0.2	6.0×10^{-9}	3.9
Heat 2	Y046-9	0.5	2.1×10^{-8}	3.8
Heat 3	D535-5	0.5	9.0×10^{-9}	4.2
Heat 3	D535-6	0.2	4.0×10^{-8}	3.3
Heat 3	K236-2F	0.5	6.3×10^{-9}	4.3

Comparison of da/dN vs. ΔK data can demonstrate the relative sensitivity of materials to hydrogen embrittlement, however such comparisons do not enable quantitative design-life evaluations of hydrogen containment structures. The da/dN vs. ΔK relationship must be used in conjunction with structural analysis to establish the design life of a hydrogen containment component. This fatigue crack growth-based design-life evaluation is specified in ASME Article KD-10 for hydrogen containment vessels. The basic objective of the design-life calculation is depicted schematically in Fig. 2.

The design-life calculation concept in Fig. 2 is based on the assumption that a hydrogen containment component (e.g., a

pressure vessel) contains an existing flaw on the interior surface (with a depth dimension, a_0), and this flaw propagates principally under the action of pressure cycles (i.e., wall stress cycles). The intent of the design-life analysis is to calculate the crack depth (a) as a function of the number of pressure cycles (N). The basic element of the design-life calculation is the fatigue crack growth law (e.g., Eq. (1)). Based on the applied pressure range and component dimensions, the stress-intensity factor range, ΔK , can be calculated at the instantaneous crack depth. This ΔK value is input into the fatigue crack growth law to calculate an increment of crack growth for the pressure cycle. The crack depth is then updated, and a new ΔK value and increment of crack growth can be calculated. This series of calculations leads to the construction of the crack depth vs. number of cycles curve in Fig. 2. The curve is truncated at a critical crack depth (a_c) associated with the onset of a new failure mode characterized by rapid crack extension.

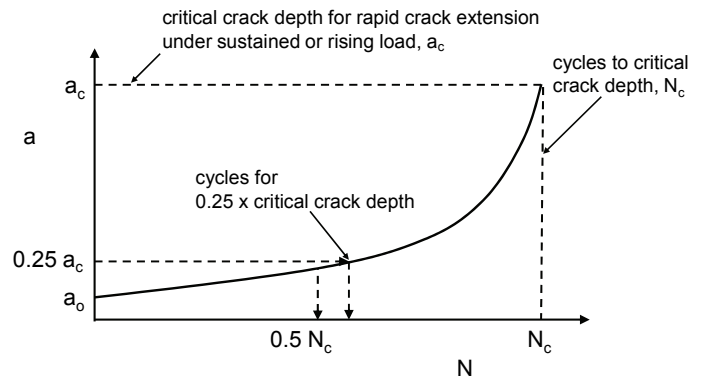


FIG. 2 SCHEMATIC OF CALCULATED CRACK DEPTH VS. PRESSURE CYCLES FOR HYDROGEN PRESSURE VESSEL

The fatigue crack growth-based design-life analysis reflected in Fig. 2 is an effective approach for assuring the safety of hydrogen containment structures that are susceptible to hydrogen embrittlement and subjected to pressure cycling. Once the crack depth vs. number of pressure cycles curve is constructed, a limiting number of pressure cycles can be imposed on the structure. For example, the ASME Article KD-10 identifies the limiting number of pressure cycles as the lower value of either 50% of the number of cycles at the critical crack depth (N_c) or the number of cycles to reach 25% of the critical crack depth (see Fig. 2). The rationale for choosing these limits is to preclude the crack from extending to the point where its growth rate starts to dramatically accelerate, i.e., the point where the slope of the a vs. N curve starts to increase rapidly. Having a reliable method to calculate the crack depth as a function of service history coupled with periodic inspection allows safety margins to be established for hydrogen containment components.

CONCLUSIONS

- The fatigue crack growth relationships (da/dN vs. ΔK) were measured for three heats of ASME SA-372 Grade J steel in 100 MPa hydrogen gas at two different load ratios (R). At $R = 0.5$, fatigue crack growth rates were similar for all three steel heats, while some variation was observed at $R = 0.2$. Fatigue crack growth rates increased mildly as R increased.
- Hydrogen accelerates fatigue crack growth rates of the SA-372 Grade J steels by at least an order of magnitude relative to crack growth rates in inert environments.
- The da/dN vs. ΔK relationships measured in hydrogen gas serve as the foundation for fatigue crack growth-based design-life analyses that demonstrate the safe operation of hydrogen containment components.

ACKNOWLEDGMENTS

The authors acknowledge J. Felbaum for supplying the test specimens and K. Lee for assistance in conducting the fatigue crack growth tests in high-pressure hydrogen gas. Sandia is a multi-program laboratory operated by Sandia Corporation, a Lockheed Martin Company, for the United States Department of Energy under contract DE-AC04-94AL85000.

REFERENCES

1. Rana, M.D., Rawls, G.B., Sims, J.R. and Upitis, E., 2007, "Technical Basis and Application of New Rules on Fracture Control of High Pressure Hydrogen Vessel in ASME Section VIII, Division 3 Code", PVP2007-26023, 2007 ASME Pressure Vessels and Piping Division Conference, ASME, New York.
2. Sims, J.R., 2012, "Standards and Codes to Control Hydrogen-Induced Cracking in Pressure Vessels and Pipes for Hydrogen Gas Storage and Transport", *Gaseous Hydrogen Embrittlement of Materials in Energy Technologies*, R.P. Gangloff and B.P. Somerday, eds., Woodhead Publishing Ltd., pp. 177-192, Cambridge, UK.
3. ASTM E647-05, 2005, "Standard Test Method for Measurement of Fatigue Crack Growth Rates", ASTM International, West Conshohocken, PA.
4. Nibur, K.A. and Somerday, B.P., 2012, "Fracture and Fatigue Test Methods in Hydrogen Gas", *Gaseous Hydrogen Embrittlement of Materials in Energy Technologies*, R.P. Gangloff and B.P. Somerday, eds., Woodhead Publishing Ltd., pp. 195-236, Cambridge, UK.

